

## The low-energy excitation spectrum of one-dimensional dipolar quantum gases

S. De Palo,<sup>1</sup> E. Orignac,<sup>2,3</sup> R. Citro,<sup>4,5</sup> and M. L. Chiofalo<sup>6,7</sup><sup>1</sup>DEMOCRITOS INFN-CNR and Dipartimento di Fisica Teorica, Università di Trieste, Trieste, Italy<sup>2</sup>Université de Lyon, Lyon, France<sup>3</sup>Laboratoire de Physique de l'École Normale Supérieure de Lyon, CNRS-UMR 5672, Lyon, France<sup>4</sup>Dipartimento di Fisica "E. R. Caianiello" and CNISM, Università degli Studi di Salerno, Salerno, Italy<sup>5</sup>LPM<sup>2</sup>C, CNRS, Grenoble, France<sup>6</sup>INFN, Dpt. of Mathematics and Faculty of Pharmacy, University of Pisa, Pisa, Italy<sup>7</sup>Classe di Scienze, Scuola Normale Superiore, Pisa, Italy

We determine the excitation spectrum of a bosonic dipolar quantum gas in a one-dimensional geometry, from the dynamical density-density correlation functions simulated by means of Reptation Quantum Monte Carlo techniques. The excitation energy is always vanishing at the first vector of the reciprocal lattice in the whole crossover from the liquid-like at low density to the quasi-ordered state at high density, demonstrating the absence of a roton minimum. Gaps at higher reciprocal lattice vectors are seen to progressively close with increasing density, while the quantum state evolves into a quasi-periodic structure. The simulational data together with the uncertainty-principle inequality also provide a rigorous proof of the absence of long-range order in such a super-strongly correlated system. Our conclusions confirm that the dipolar gas is in a Luttinger-liquid state, significantly affected by the dynamical correlations. The connection with ongoing experiments is also discussed.

**Introduction.**— Ultracold quantum gases with dipolar interactions are currently being produced in laboratory, where atomic  $^{52}\text{Cr}$  atoms have been Bose-condensed [1, 2], following earlier theoretical predictions [3, 4]. Experiments have been suggested [5] aimed to produce molecular gases with large dipolar strengths, and a few laboratories worldwide are working along these lines. In fact, dipolar quantum gases are emerging as competitive realizations of quantum devices [6] and as a laboratory for investigating strongly correlated regimes [7, 8] and novel quantum phases [9, 10], in which quantum fluctuations are enhanced by exploiting techniques acquired for an accurate manipulation of atomic gases. These include the possibility of lowering the temperature; of tuning the interactions in both their long-range tail [11] and in the strength of their short-range part [12] by means of the Fano-Feshbach mechanism [13, 14] to let emerge the dipolar character [15]; of reducing the dimensionality down to one (1D), as already performed in other systems [16, 17].

One-dimensional quantum gases are naturally inclined to be strongly correlated [18–29]. We have more recently predicted that dipolar bosonic quantum gases confined in quasi-1D geometries can reach correlation regimes well beyond those of the (already strongly correlated) Tonks-Girardeau (TG) gas [19], crossing over to a Dipolar-Density-Wave (DDW) state at very large densities  $n$  on the scale of the potential range, where the atoms arrange into an ordered state regularly spaced by  $n^{-1}$  [30]. By a back-to-back comparison with Reptation Quantum Monte Carlo (RQMC) [20] simulational data, we have shown that at the level of the static structure factor the crossover can be described by a Luttinger-liquid theory with exponent  $K < 1$  continuously decreasing from  $K = 1$  at  $n \rightarrow 0$  to  $K \rightarrow 0$  as  $n \rightarrow \infty$ . Finally, we have predicted the corresponding signatures in the collective excitations of the trapped gas [21].

Beyond the evidence emerging from the static struc-

ture of the fluid, a clear-cut demonstration of Luttinger behavior requires further understanding of the excitations in the homogeneous dipolar gas. In particular, answers to two relevant questions are not obvious from the beginning. First, whether roton-like excitations may show up in the dipolar gas at finite wavevectors. Second, whether the quantum fluctuations of the phonon field prevent the existence of long-range order at large densities, namely whether the crystal order parameter vanishes in the thermodynamic limit. In fact, exploiting the uncertainty-principle instead of the Bogolubov inequality, Pitaevskii and Stringari [22] have worked out an extension of the Hohenberg-Mermin-Wagner theorem [23, 24] which yields more accurate upper bounds to the size of the order parameter at zero temperature, where the quantum fluctuations dominate. When applied to specific systems, the inequality may allow to rule out the existence of long-range order, as in the case of, e.g., 1D antiferromagnets and crystals [22]. Both questions above would have a definite answer if the system were in a Luttinger-liquid state, for which there is no long-range order nor roton minimum.

In this Brief Report, we find that this is indeed the case, after computing by RQMC the low-energy excitation spectrum up to eight reciprocal lattice vectors  $G_m = n = 2\pi m$  in the whole crossover. The evolution of quasi-long-range order from the TG to the DDW state emerges as a progressive closing of the gaps in the excitation spectrum with increasing the order  $m$ . By the same token, we demonstrate the absence of a roton minimum at  $2\pi$  in the whole crossover and that dynamical effects play a significant role in building the Luttinger state. Our results, analyzed by means of the uncertainty-principle inequality [22], also rule out the existence of long-range order in this super-strongly correlated quantum gas and confirm that the 1D dipolar gas is in a Luttinger-liquid state.

The model and the RQMC method.— We model the 1D dipolar Bose gas by considering  $N$  atoms with mass  $M$  and permanent dipoles moments arranged along and orthogonal to a line, yielding purely repulsive interactions. The Hamiltonian is

$$H = \frac{1}{2} \sum_i \frac{\partial^2}{\partial x_i^2} + \frac{1}{2} \sum_{i < j} \frac{1}{|x_i - x_j|^3} : \quad (1)$$

in effective Rydberg units  $Ry = \hbar^2/(2M r_0^2)$ . The effective Bohr radius  $r_0 = M C_{dd}/(2 \hbar^2)$  is expressed in terms of the interaction strength  $C_{dd} = \int_0^\infty \frac{d^2}{d^2}$  for magnetic and  $C_{dd} = d^2/\epsilon_0$  for electric dipoles [31]. The dimensionless parameter  $r_s = 1/(nr_0)$  determines the interacting regime in terms of  $r_0$  and of the linear density  $n$ . Since the potential-to-kinetic energy ratio scales as  $1/r_s = nr_0$ , large densities yield to strong correlations, at variance with Coulomb systems.

We determine the ground-state properties and the excitation spectrum by resorting to the Reptation Quantum Monte Carlo technique [20]. This is in essence a path-integral method at zero temperature, where the ground-state distribution is directly sampled in the internal part of the path. Thus, the computation of the structure of the uid and of the imaginary-time correlation functions for suitable long projection times is conceptually straightforward and practically easy, since possible biases arising from mixed averages are ruled out by definition. In particular, from an analysis of the imaginary-time density-density correlation function we determine the low-energy excitation spectrum while the parameter  $nr_0$  spans the whole crossover from the TG to the DDW state.

We use a trial wave-function that is a product of two-body Jastrow factors  $\psi_{\text{trial}} = \prod_{i < j} e^{u(z_i, z_j)}$ . As we are interested in long-range behavior, we actually take the Luttinger-liquid expression

$$\psi_{\text{trial}}(R) / \prod_{i < j} \sin \frac{\pi}{L} (x_i - x_j)^{1/K} : \quad (2)$$

which in the low-density limit implies  $K = 1$  [7] and recovers the wave-function of spinless non-interacting fermions. Different choices of the wave functions, such as the product of gaussians centered on the lattice sites  $R_m = m n^{-1}$ , result into different time-step extrapolations, but eventually lead to negligible differences in the computation of the static and dynamic structure factors.

A few technical details are in order. We perform simulations for different values of the number  $N$  of bosons in a square box with periodic boundary conditions, namely  $N = 40; 60; 80; 100$ , reaching in selected cases  $N = 200$ . We check that we are able to take care of finite-size effects by summing the interactions over ten simulation boxes. Finally, the energies are extrapolated to their thermodynamic limit after removing the time-step dependence.

The resulting energy per particle  $\epsilon(nr_0) = Ry$  as a function of  $nr_0$  has been provided in [21, 25], together with an accurate analytical form of it, useful for further applications. We remark here that  $\epsilon(nr_0) = Ry$  recovers the

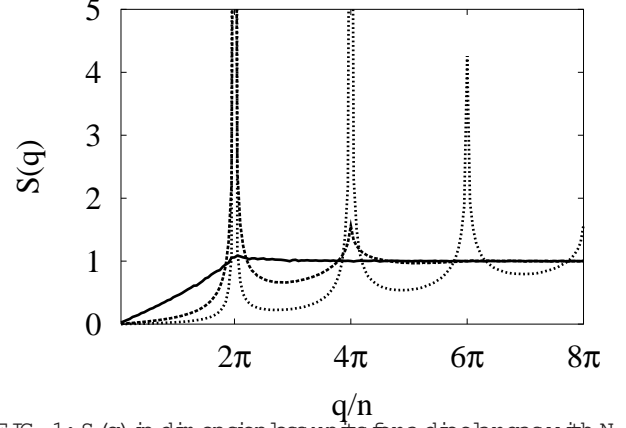


FIG. 1:  $S(q)$  in dimensionless units for a dipolar gas with  $N = 40$  particles and different values of  $nr_0 = 0.01; 50$  and  $1000$ . Decreasing slopes as  $q \rightarrow 0$  and the emergence of additional peaks correspond increasing  $nr_0$  values.

known limiting behaviors  $\epsilon(nr_0) = Ry$  ( $\epsilon = 3$ )  $(nr_0)^2$  for  $nr_0 \rightarrow 1$  in the TG regime and  $\epsilon(nr_0) = Ry$  ( $\epsilon = 3$ )  $(nr_0)^3$  for  $nr_0 \rightarrow 1$  in the DDW limit [7]. We set from now on units of  $n^{-1}$  for lengths and of  $Ry$  for energies.

Low energy excitations from dynamical structure factor.— We determine the low-energy excitations after computing the imaginary-time correlation function of the density operator [26]  $\rho_q = \prod_i \exp(iq \cdot r_i)$  creating a density fluctuation with wave vector  $q$ , that is  $F(q; \tau) = \langle \rho_q(\tau) \rho_q(0) \rangle / N$ , where the sum in  $q$  spans over the number of particles  $N$  located at position  $r_i$  and  $\tau$  is the imaginary time.  $F(q; \tau)$  is related to the dynamical structure factor by  $F(q; \tau) = \int_0^\infty d\omega e^{-\omega \tau} S(q; \omega)$ , yielding the static structure factor for  $\tau = 0$ , namely  $S(q) = F(q; 0) = \int_0^\infty d\omega S(q; \omega)$ .

To give a system overview, we first display the  $S(q)$  in Fig. 1 as previously determined [7] by RQMC for various densities between the TG and DDW limits. Peaks at  $q/n = 2\pi m$  ( $m$  integer) progressively disappear with decreasing density as the dipolar gas approaches the spinless fermionic liquid.

We track this smooth evolution by investigating the low-energy excitations as extracted from the dynamical structure factor  $S(q; \omega)$ . From the expression

$$S(q; \omega) = \sum_n \langle \rho_{q-n} \rho_{n-q} \rangle e^{i\omega \tau} : \quad (3)$$

we estimate the energy dispersion of the collective excitations by fitting the imaginary-dependence of  $F(q; \tau)$  as a sum of exponentials  $\sum_i A_i(q) e^{-\epsilon_i(q) \tau}$  corresponding to multiple modes. Then, the  $\chi^2$  yielding the best  $\chi^2$  value is chosen.

Fig. 2 displays the resulting RQMC energy dispersion  $\epsilon(q)$ , for the case with  $N = 40$  at  $nr_0 = 1; 10$  and  $1000$  namely in the low, intermediate and very high density regimes. In spite of the finite size effects, the overall qualitative behavior is already clear. The phonon softens at low  $q$ -values, while the density decreases. On the

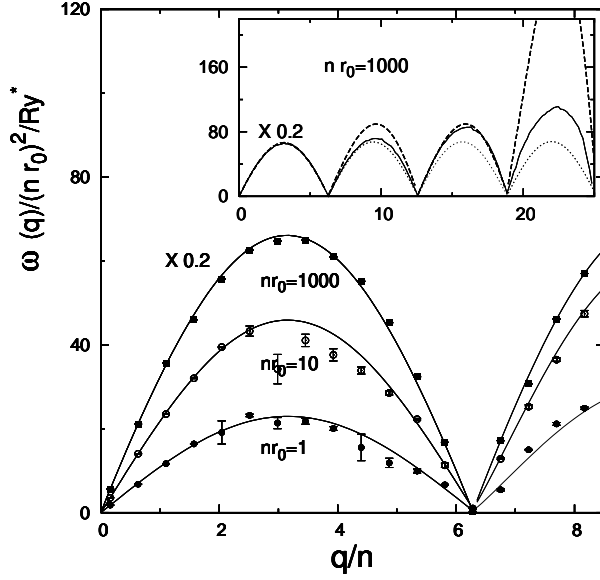


FIG. 2: Lowest excitation energies  $\omega(q)$  in Ry units and scaled by  $(nr_0)^2$ , for a dipolar gas with  $N = 40$  and different values of  $nr_0 = 1; 10$  and  $1000$  as in the legend. Symbols with error bars represent the RQMC data extracted from (3), the solid line is a guide to the eye. The curve at  $nr_0 = 1000$  is depressed by a factor of 5 for graphical reasons. Inset: zoom on the  $\omega(q)$  at  $nr_0 = 1000$  up to  $q/n = 8$  for different  $F(q)$  models: multimode (solid) and Feynman (dashed) approximation. Dotted line: periodic replica of the first bump.

other hand, the gap at  $2\pi$  seems to be always closed at all densities. As represented in the inset by the dotted curve, even at  $nr_0 = 1000$  the RQMC excitation spectrum (solid line) is very different from what could be obtained by replicating the portion from  $q = 0$  to  $q = 2\pi$  (dotted line), indicating a non periodic structure. The dashed line instead, represents  $\omega(q)$  obtained from the Feynman relation  $\omega(q) = \omega(q) = S(q)$ , which provides only an upper bound to  $\omega(q)$  in terms of the static structure factor  $S(q)$  and of the kinetic energy  $\omega(q) = \hbar^2 q^2 / 2m$ . Indeed, the Feynman relation is clearly seen to overestimate the RQMC value for  $q > 2\pi$ , while it seems to account for the  $\omega(q)$  between  $q = 0$  and  $q = 2\pi$ . Considering that the Feynman relation is expected to yield better results as  $q \rightarrow 0$ , we can also anticipate that at lower densities the  $q$  range where the Feynman relation is reliable will shrink (see below).

A quantitatively reliable measure of the gap sizes requires an accurate size effect analysis. Fig. 3 displays the  $1/N$  scaling of  $\omega(q=2\pi)$  for  $nr_0 = 0.01; 0.1; 1; 10$  and  $1000$ . The fit to the RQMC data (symbols in the figure) yields the linear scaling  $\omega(q=2\pi) = c(nr_0)/N$  with the constant  $c(nr_0)$  being an increasing function of  $nr_0$ . Thus,  $\omega(q=2\pi) \rightarrow 0$  as  $1/N \rightarrow 0$ , the gap is clearly closed at all densities, demonstrating the absence of a roton minimum. This is not the case if we use the

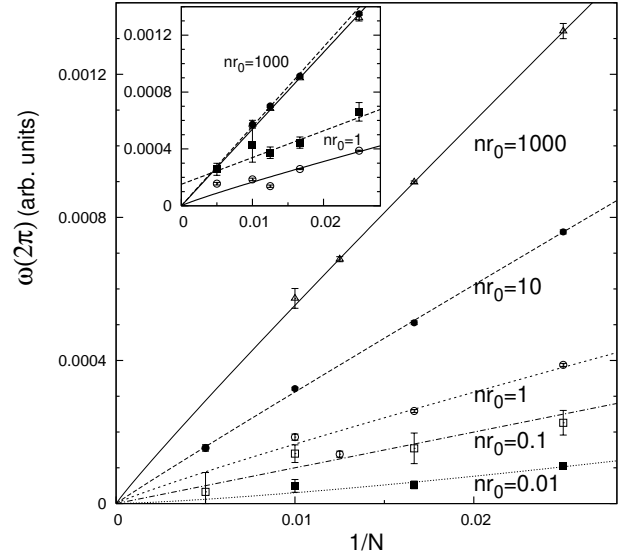


FIG. 3:  $1/N$  scaling of  $\omega(q=2\pi)$  in arbitrary units at  $nr_0 = 0.01; 0.1; 1; 10$  and  $1000$  as in the legend. Symbols with error bars: RQMC data. Solid lines: fit to the data. Inset: zoom of the RQMC data and related fits for the cases with  $nr_0 = 1$  and  $1000$ . Filled symbols and dashed lines: Feynman relation (single-mode approximation). Open symbols and solid lines: two-mode analysis yielding the best fit.

Feynman relation, corresponding to a single-mode approximation in Eq. (3) [20]. At the intermediate-to-low density  $nr_0 = 1$  the fit yields a finite gap value (see the inset). Since the Feynman relation is built up from static quantities, we may conclude that dynamical effects, as embodied in the multimode analysis of (3) play a significant role, leading to qualitatively different conclusions. A similar multimode analysis performed at  $q = 2\pi$ ,  $m > 2$  shows the existence of open gaps, which progressively close while the quasi-ordered state is approached.

Absence of long-range order.— Using these results, we can derive a strict upper bound for the order parameter of the solid  $\rho_s = N^{-1} \hbar^2 \sum_{\mathbf{q}} \exp(i\mathbf{G} \cdot \mathbf{r}_i) \langle \mathbf{r}_i | \mathbf{r}_j \rangle$  with  $\mathbf{G}$  a vector of the reciprocal lattice, and rigorously test the qualitative conclusions from the inset of Fig. 2, namely that no long-range order may exist in our 1D dipolar quantum gas. We closely follow the derivation of Pitaevskii and Stringari [22]. By applying the uncertainty-principle inequality  $\langle \mathbf{A}^\dagger \mathbf{A} \rangle \langle \mathbf{B}^\dagger \mathbf{B} \rangle \geq |\langle \mathbf{A}^\dagger \mathbf{B} \rangle|^2$  to the operators  $\mathbf{A} = \sum_{\mathbf{q}} \hat{a}_{\mathbf{q}+\mathbf{G}}$  and  $\mathbf{B} = \sum_{\mathbf{q}} \hat{a}_{\mathbf{q}} \exp(i\mathbf{G} \cdot \mathbf{r}_i)$  one has  $S(\mathbf{q}+\mathbf{G}) \geq \frac{1}{4m^2} \frac{1}{G^2} \langle \mathbf{q} | \mathbf{q} + \mathbf{G} \rangle^2$ . From the RQMC data we know that as  $q \rightarrow 0$ ,  $S(\mathbf{q}+\mathbf{G}) \rightarrow \frac{1}{4m^2} \frac{1}{G^2} \langle \mathbf{q} | \mathbf{q} \rangle^2$ , while the second moment of  $S(\mathbf{q};!)$  vanishes as  $\frac{1}{4m^2} \frac{1}{G^2} \langle \mathbf{q} | \mathbf{q} \rangle^2$ . Thus, the order parameter in the long wavelength limit vanishes as  $\frac{1}{G^2} \langle \mathbf{q} | \mathbf{q} \rangle^2 \propto \frac{1}{K^2}$  with  $K \rightarrow 0$ . Thus no long-range order may exist unless  $K = 0$ , which is however the limit of infinite density.

Dynamical response function and Luttinger-liquid analysis.— These results can be analyzed within the

Luttinger-liquid theory. We want to calculate the imaginary-time correlation function  $F^*(x; \tau) = \langle T e^{i2\pi(x; \tau)} \rangle_{i,0}$ , on a finite size system of length  $L$ . It is known [27] from bosonization that  $F^*(x; \tau) = (\tau/L)^{2K} = \sinh^2 \frac{u}{L} + \sin^2 \frac{x}{L}^K$  valid in the long-time (low-energy) limit where  $\tau$  is a short-distance cutoff of the order of  $\tau^{-1}$ ,  $u$  is the velocity of the excitations and  $K$  the Luttinger exponent. After Fourier transforming  $F^*(x; \tau)$  in  $q$ -space with  $q = 2\pi j/L$ , we get:

$$F(q; \tau) = \frac{1}{L} \sum_{j=0}^{2K} \frac{e^{-\frac{2u}{L}(K+j)\tau}}{1 + e^{-\frac{2u}{L}(K+j)\tau}}$$

$$[(j+K)][(K-j)(j+1)]^{-1} {}_2F_1(K+j; K; j+1; e^{-\frac{2u}{L}\tau})$$

where  ${}_2F_1$  and  $\Gamma$  are the Hypergeometric and Euler functions.

Using an Ansatz  $e^{-\frac{2u}{L}(K+j)\tau}$  to fit the long-time behavior  $F(q; \tau) \sim \tau^{-2u/K}$  we get  $\frac{2u}{L} = 2 - u/K$  where we have used the even parity of the response function. Thus, there should be no roton gap at  $q = 2\pi/L$  in the infinite size limit. For finite size, an apparent roton gap (vanishing as  $1/L$ ) can be seen. This gap can be traced to the zero mode contribution to the correlation functions. All the fits to the RQM C data presented in

Figs. 2-3 reproduce remarkably well this  $1/L$  scaling [32], and are consistent with our previous findings on the density dependence of Luttinger-K exponent  $K(n)$  [7].

Conclusions.— In conclusion, the analysis of the RQM C simulational data neatly lead to two main conclusions, namely that there are no roton excitations appearing at the first star of the reciprocal lattice and that no long range order may exist in the whole crossover from the TG gas at low density to the quasi-ordered DDW state at high densities. The RQM C data analysis is in remarkable agreement with what expected for a super-strongly correlated Luttinger-liquid state, with the inclusion of significant dynamical effects. The realization of 1D dipolar quantum (molecular) gases in the TG to the DDW regime is within reach of current experimental efforts [7] and thus our predictions on the excitation spectrum and on the absence of the roton minimum, can be tested in future experiments by means of e.g. Bragg spectroscopy techniques [28].

Acknowledgments. We are especially grateful to the Scuola Normale Superiore to have provided ideal conditions for the realization of large parts of this work, and to G. La Rocca for interesting discussions and support. We also thank S. Stringari and L. Pitaevskii to have pointed out the use of the uncertainty-principle inequality.

- 
- [1] J. Stuhler, A. Griemaler, T. Koch, M. Fattori, T. Pfau, S. Giovanazzi, P. Pedri, and L. Santos, Phys. Rev. Lett. 95, 150406 (2005).
- [2] A. Griemaler, J. Wemer, S. Hensler, J. Stuhler, and T. Pfau, Phys. Rev. Lett. 94, 160401 (2005).
- [3] L. Santos, G. V. Shlyapnikov, P. Zoller, and M. Lewenstein, Phys. Rev. Lett. 85, 1791 (2000).
- [4] K. Goral, K. Rzaewski, and T. Pfau, Phys. Rev. A 61, 051601 (2000).
- [5] H. P. Buchler et al. (2006), cond-mat/0607294.
- [6] P. Rabl and P. Zoller (2007), arXiv:0706.3051v1 [quant-ph].
- [7] R. Citro, E. Orignac, S. D. Palo, and M. L. Chiofalo, Phys. Rev. A 75, 051602R (2007).
- [8] A. S. Arkhipov, G. E. Astrakharchik, A. V. Belikov, and Y. E. Lozovik, JETP Lett. 82, 39 (2005).
- [9] K. Goral, L. Santos, and M. Lewenstein, Phys. Rev. Lett. 88, 170406 (2002).
- [10] H. Pu, W. Zhang, and P. Meystre, Phys. Rev. Lett. 87, 140405 (2001).
- [11] S. Giovanazzi, A. G. Orlicz, and T. Pfau, Phys. Rev. Lett. 89, 130401 (2002).
- [12] T. Lahaye, T. Koch, B. Frohlich, M. Fattori, J. Metz, A. Griemaler, S. Giovanazzi, and T. Pfau, Nature (2007), in press.
- [13] H. Feshbach, Ann. Phys. 5, 357 (1958).
- [14] U. Fano, Phys. Rev. 124, 1866 (1961).
- [15] S. Ronen, D. C. E. Bortolotti, D. Blum, and J. L. Bohn, Phys. Rev. A 74, 033611 (2006).
- [16] B. Paredes, A. Wildera, V. Murg, O. Mandel, S. Fölling, I. Cirac, G. V. Shlyapnikov, T. W. Hansch, and I. Bloch, Nature 429, 277 (2004).
- [17] T. Kinoshita, T. Wenger, and D. S. Weiss, Science 305, 5687 (2004).
- [18] T. Giamarchi, Quantum Physics in One Dimension (Oxford University Press, Oxford, UK, 2004).
- [19] M. Girardeau, J. Math. Phys. 1, 516 (1960).
- [20] S. Baroni and S. Moroni, Phys. Rev. Lett. 82, 4745R (1999).
- [21] P. Pedri, S. D. Palo, E. Orignac, R. Citro, and M. L. Chiofalo, cond-mat/0708.2789 (2007), submitted.
- [22] L. Pitaevskii and S. Stringari, J. of Low Temp. Phys. 85, 377 (1991).
- [23] N. D. Mermin and H. Wagner, Phys. Rev. Lett. 17, 1133 (1966).
- [24] P. C. Martin, Phys. Rev. 158, 383 (1967).
- [25] R. Citro, S. D. Palo, P. Pedri, E. Orignac, and M. L. Chiofalo (2007), in preparation.
- [26] S. D. Palo, S. Conti, and S. Moroni, Phys. Rev. B 69, 035109 (2004).
- [27] T. Giamarchi, Quantum Physics in One Dimension (Oxford University Press, Oxford, 2004).
- [28] D. M. Stamper-Kurn, A. P. Chikkatur, A. G. Orlicz, S. Inouye, S. Gupta, D. E. Pritchard, and W. Ketterle, Phys. Rev. Lett. 83, 2876 (1999).
- [29] Thus, 1D dipolar quantum gases are amenable to a variety of interesting effects, as e.g. spin-charge separation (see A. Kleine and C. Kollath and I. M. Cullloch and T. Giamarchi and U. Schollwoeck, arXiv:0706.0709 (2007)).
- [30] By dipolar-density-wave we mean a quasi-ordered state very much analogous to a charge-density-wave.
- [31]  $d$  and  $d$  are the magnetic and electric dipole moments

and  $\epsilon_0$  and  $\mu_0$  are the vacuum permittivities

[32] At fixed density,  $1=N$  and  $1=L$  scaling are equivalent.